Ferroelectric Soft Mode in a $SrTiO_3$ Thin Film Impulsively Driven to the Anharmonic Regime Using Intense Picosecond Terahertz Pulses

I. Katayama,[1] H. Aoki,[2] J. Takeda,[2] H. Shimosato,[3] M. Ashida,[3,4] R. Kinjo,[5] I. Kawayama,[5] M. Tonouchi,[5] M. Nagai,[4,6] and K. Tanaka[6,7,8]

[1]*Interdisciplinary Research Center, Yokohama National University, Yokohama 240-8501, Japan*
[2]*Graduate School of Engineering, Yokohama National University, Yokohama 240-8501, Japan*
[3]*Graduate School of Engineering Science, Osaka University, Toyonaka 560-8531, Japan*
[4]*PRESTO JST, Tokyo 102-0075, Japan*
[5]*Institute of Laser Engineering, Osaka University, Suita 565-0871, Japan*
[6]*Graduate School of Science, Kyoto University, Kyoto 606-8502, Japan*
[7]*iCeMS, Kyoto 606-8501, Japan*
[8]*CREST JST, Tokyo 102-0075, Japan*

(Received 7 April 2011; revised manuscript received 2 October 2011; published 28 February 2012)

The ferroelectric soft mode in a $SrTiO_3$ thin film was impulsively driven to a large amplitude using intense picosecond terahertz pulses. As the terahertz electric field increased, the soft-mode absorption peak exhibited blueshifting and spectral narrowing. A classical anharmonic oscillator model suggests that the induced displacement is comparable to that of the ferroelectric phase transition. The spectral narrowing indicates that the displacement exceeds that induced by any inhomogeneities in the film, demonstrating that the method can be used to explore intrinsic quartic anharmonicity.

DOI: 10.1103/PhysRevLett.108.097401 PACS numbers: 78.47.jh, 42.65.Sf, 63.20.Ry, 77.55.−g

Recent developments in ultrashort laser pulse technologies have enabled unique methods for coherent manipulation of the phases and properties of condensed matter [1]. In particular, since ionic and molecular motion in solids typically occurs on the picosecond time scale, the intense femtosecond laser pulses can be used to impulsively drive these motions to large amplitudes far from thermal equilibrium [2]. This mechanism has a wide range of applications, particularly in selective chemical reactions [3] and ultrafast coherent switching of macroscopic phases [4].

Large-amplitude vibrations are commonly induced via electronic excited states or by impulsively stimulated Raman scattering processes [5,6], which are second- or higher-order processes of the incident electromagnetic field. In these processes, the envelope function of the electric field of the laser pulse drives picosecond vibrations in materials. However, a resonant low-frequency electromagnetic pulse can directly drive large-amplitude displacements in infrared-active modes more efficiently than an ultrashort optical pulse because the driving force is proportional to the electric field, whose oscillation period matches the time scale of the vibration. This alternative also allows greater control for a *cleaner* experiment, i.e., one without unexpected electronic excitation such as photoinduced damage to the material.

Since excitations associated with macroscopic phase transitions exist in the terahertz region, many efforts are being made to demonstrate terahertz-induced macroscopic phase transformations with few-cycle terahertz pulses. A further motivation is the recent theoretical prediction that phase-controlled terahertz pulse excitation can flip the ferroelectric polarization [7]. Indeed, softening of the intermolecular modes in organic crystals has already been experimentally demonstrated [8]. However, the large potential barriers to structural phase transitions in these systems require terahertz pulses with an impractically large electric field.

$SrTiO_3$ thin films, however, have low potential barriers to ferroelectric phase transitions. This is because the extrapolated Curie temperature for the ferroelectric phase transition in $SrTiO_3$ is comparable to the energy of terahertz photons [9]. Small perturbations such as those from an external electric field, uniaxial pressure, or isotope or impurity substitutions are known to induce ferroelectric phase transitions in this material [10–12]. The material has a highly anharmonic soft mode associated with these properties [see Fig. 1(a)] with an extremely large oscillator strength in the terahertz region at low temperature [13,14]. Thus, it is particularly suited to a demonstration of coherent control of ferroelectric polarization.

In this study, we focus on the soft mode in a $SrTiO_3$ thin film in order to demonstrate coherent driving of large-amplitude ferroelectric polarization. Our results demonstrate for the first time that intense picosecond terahertz pulses can impulsively drive the dipole-allowed ferroelectric soft mode in a $SrTiO_3$ thin film to the anharmonic region, where the amplitude is comparable to that of the ferroelectric distortion expected in the perturbation-induced ferroelectric phase. In addition, the induced displacement of the soft mode appears to exceed that induced by any inhomogeneities in the thin film. Thus, the intrinsic anharmonicity of the soft mode at low temperature can

 © 2012 American Physical Society

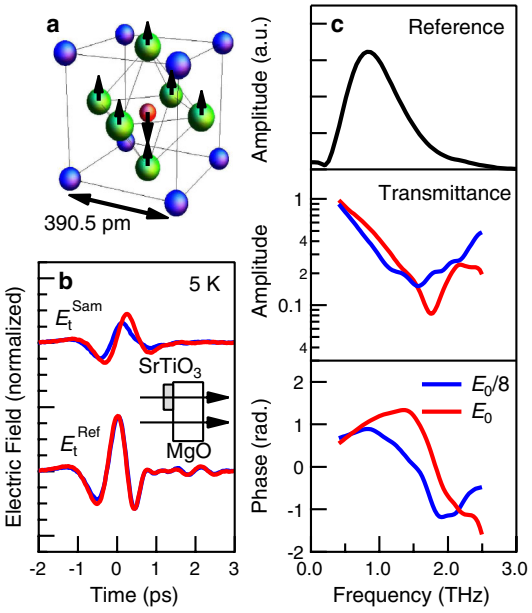

FIG. 1 (color online). (a) Schematic representation of the crystal structure (perovskite structure) and soft-mode oscillation (Slater mode) in $SrTiO_3$. (b) Field dependence of the transmitted waveform for a 300-nm-thick $SrTiO_3$ thin film sample deposited on MgO at 5 K. The reference waveform (MgO substrate) is also plotted. Red lines represent the data at $E_0 = 80$ kV/cm; blue lines represent those at $E_0/8$. Each amplitude is normalized by the respective reference amplitude. (c) Amplitude and phase of the complex transmittance of the $SrTiO_3$ thin film calculated from the data shown in Fig. 1(b). The spectrum of the reference waveform (MgO substrate) is also plotted.

be quantitatively estimated by this method. Our results demonstrate the strong potential of terahertz pulses for coherent control of macroscopic phases in materials and also for nonlinear terahertz spectroscopy. In addition, evaluation of the anharmonic potential could be important for understanding the lattice dynamics and local vibrational potential of ferroelectric or quantum paraelectric materials.

The samples were 300-nm-thick $SrTiO_3$ thin films deposited on a 0.5-mm-thick MgO substrate using pulsed laser deposition [15]. They were post-annealed at 1300 °C for 12 h to improve the crystallinity [16]. Their linear terahertz absorption spectrum showed that the soft mode undergoes spectral broadening and hardening possibly because of spatial inhomogeneities [16,17]. Although a strong lattice mismatch exists between the $SrTiO_3$ ($a = 3.905$ Å) and the MgO substrate ($a = 4.213$ Å), annealing reduces the misfit strain from the substrate. As a result, the extrapolated Curie temperature derived from the temperature dependence becomes approximately 0 K, compared with 35.5 K for the bulk crystal, which still indicates large anharmonicity [9,16,18]. In addition, a simple evaluation of the nonlinear polarization of a film can be performed without considering the complicated nonlinear propagation equation for electromagnetic waves in the medium.

For the laser, we used the output of a 1-kHz regenerative amplifier seeded with a frequency-doubled fiber laser oscillator. The wavelength, energy, and pulse duration of the laser were 780 nm, 0.56 mJ, and 150 fs, respectively. We generated intense terahertz pulses using a Mg-doped $LiNbO_3$ single crystal excited by laser pulses having tilted pulse fronts [19–22]. The generated terahertz waves were collimated and focused on the sample and on an electro-optic (EO) crystal by four parabolic mirrors. The maximum terahertz electric field at the sample was 80 kV/cm, and the terahertz waves were polarized parallel to the (100) axis of the MgO substrate. The EO crystal was a 1-mm-thick ZnTe crystal used to measure the waveform of the terahertz pulses. The sample was cooled using a He-flow cryostat, whose temperature could be controlled from 5 K to room temperature. We mounted the sample between two wire-grid polarizer pairs and changed the field amplitude at the sample without changing the incident pulse profile, the polarization at the sample, and the field amplitude at the EO crystal.

Figure 1(b) shows typical experimental results of the terahertz waveforms passing through the sample. Although the reference waveforms $E_t^{\mathrm{Ref}}(t)$ transmitted through the MgO substrate show little change with increasing electric-field amplitude, those transmitted through the $SrTiO_3$ thin film, $E_t^{\mathrm{Sam}}(t)$, show two clear and characteristic changes: the amplitude increases, and the oscillation period decreases. These changes originate from the nonlinear responses of the $SrTiO_3$ thin film.

We calculated the complex transmittances in the frequency domain from the waveforms in Fig. 1(b) [see Fig. 1(c)]. The complex transmittance $t(\omega)$ is defined as the ratio of the terahertz spectrum passing through a sample $[E_t^{\mathrm{Sam}}(\omega)]$ to that passing through the substrate $[E_t^{\mathrm{Ref}}(\omega)]$, that is, $t(\omega) = E_t^{\mathrm{Sam}}(\omega)/E_t^{\mathrm{Ref}}(\omega)$. At low amplitude ($E_0/8$), the transmission spectrum shows strong absorption at 1.5 THz, which corresponds to the resonant frequency of the soft mode. However, at higher amplitude (E_0), the absorption frequency blueshifts to 1.8 THz, demonstrating the anharmonicity of the soft mode. In addition, the strength of the absorption at the resonant frequency increases with the magnitude of the terahertz field.

Let $P(\omega)d$ denote the total polarization per unit area of the thin film. Then, the susceptibility $\chi(\omega) \equiv P(\omega)/E_{\mathrm{film}}(\omega)$ (or equivalently, the conductivity $\sigma(\omega)$) can be evaluated directly from the complex transmittance $t(\omega)$ when the thickness d is much less than the wavelength of the incident light [23,24]. We expand this definition to the case with nonlinear polarization to calculate the effective susceptibility $\chi_{\mathrm{eff}}(\omega)$ as

$$\chi_{\mathrm{eff}}(\omega) = \frac{c(n+1)(t(\omega)-1)}{i\omega t(\omega)d}. \quad (1)$$

Here, ω, n, c, ϵ_0, and E_{film} are the angular frequency, refractive index of the substrate, speed of light, permittivity of vacuum, and electric field inside the film, respectively.

We examined the real and imaginary parts of $\chi_{\mathrm{eff}}(\omega)$ for incident terahertz waves of different amplitudes (Fig. 2). The resonant frequency of the soft mode remains almost unchanged for $E_0/32$ and $E_0/8$ but shows clear high-frequency shifts for $E_0/2$ and E_0. Furthermore, the bandwidth of the absorption decreases as the incident field amplitude increases.

With increasing temperature, the soft mode in $SrTiO_3$ is known to exhibit a high-frequency shift and spectral broadening because of anharmonicity and thermal fluctuations in the soft mode and the other coupled modes, respectively [16,25]. This high-frequency shift observed at high electric-field amplitude is consistent with the temperature dependence of the soft-mode frequency. However, the trend in the spectral narrowing at high electric-field amplitude is opposite to that seen in the temperature dependence of the soft-mode frequency. This point is particularly important because it indicates that the terahertz pulse drives the soft mode and not the other modes, whereas all the phonon modes are excited equally when the temperature is increased. This targeted excitation capability makes nonlinear terahertz spectroscopy a powerful method for studying anharmonicity and nonlinear mode coupling in the terahertz region.

To elucidate the anharmonic lattice dynamics, we simulated the nonlinear response of the soft mode under an intense terahertz electric field using a classical anharmonic oscillator model [26]. Here, the soft mode is considered as a single mode at the Γ point because the terahertz pulse has a smaller wave vector than those at most points in the Brillouin zone. The inhomogeneities of individual local oscillators, which stem from defects or stress from the substrate, are included in the damping constant of the soft mode. We consider the quartic term in the potential (namely, Q^3 in the force term) and numerically solve the equation to obtain the time-dependent polarization $P(t)$. The equation of motion is written as

$$\frac{d^2Q}{dt^2} + \Gamma\frac{dQ}{dt} + \Omega^2 Q + \lambda Q^3 = \frac{e^* E_{\mathrm{film}}(t)}{M}. \qquad (2)$$

Here, Ω, λ, Γ, M, and e^* are the resonant frequency, quartic anharmonicity constant, damping constant, effective mass, and effective charge of the soft mode, respectively. We used $e^* = 7.37e$ (e: electron charge) and $M = 18.6m$ (m: proton mass) according to the effective charge calculated in Ref. [27] and the oscillator strength of the soft mode observed in our sample [16].

In the thin film approximation, the driving force of the soft mode is independent of the position inside the film, because the electric field $E_{\mathrm{film}}(t)$ can be regarded as homogeneous. Thus, $E_{\mathrm{film}}(t)$ is given by [28] as

$$E_{\mathrm{film}}(t) = \frac{1}{n+1}\left(2E_i(t) - \frac{d}{\epsilon_0 c}\frac{\partial P(t)}{\partial t}\right). \qquad (3)$$

Here, $E_i(t)$ is the incident terahertz electric field, and d is the thickness of the film. The resonant frequency ($\Omega = 2\pi \times 1.4$ THz) and linear damping constant ($\Gamma_0 = 2\pi \times 0.66$ THz) are set to reproduce the linear dielectric dispersion of the film, and λ is set to fit the nonlinear change in the spectrum. The initial position of Q is the origin ($Q = 0$), which is the average of the quantum mechanical fluctuations in $SrTiO_3$. The effective susceptibility $\chi_{\mathrm{eff}}(\omega)$ can be calculated from the Fourier transforms of $P(t)$ and $E_{\mathrm{film}}(t)$.

This model reproduces the frequency shift of the soft mode at high electric-field strength but not the spectral narrowing. This is because even though the quartic anharmonicity is included, higher-order damping terms are not. Because $SrTiO_3$ exhibits inversion symmetry, the lowest order nonlinear damping should be proportional to Q^2; thus, the overall damping constant becomes $\Gamma = \Gamma_0 + \alpha Q^2$. Here, Γ_0 is the damping constant valid for the limit of small displacement, whereas α is the phenomenological nonlinear damping coefficient, which has a minus sign in order to reproduce the spectral narrowing of the soft mode. The lines in Fig. 2 show the calculated real and imaginary parts of χ_{eff} with a quartic anharmonicity $\lambda = 35\ \mathrm{pm}^{-2}\,\mathrm{THz}^2$ and a nonlinear damping coefficient of $\alpha = -3.5\ \mathrm{pm}^{-2}\,\mathrm{THz}$. The potential used for the soft mode is shown in Fig. 3(a).

The inhomogeneous broadening in the resonance of local oscillators is due to the spatially dependent stress from the substrate. The stress induces local ion displacement,

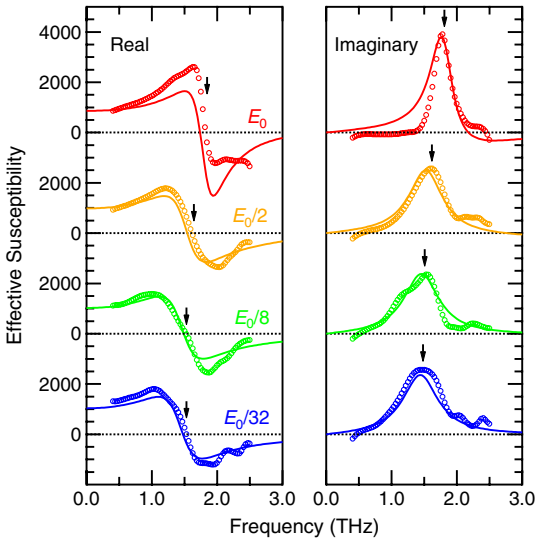

FIG. 2 (color online). Derived real and imaginary parts of effective susceptibility $\chi_{\mathrm{eff}} \equiv P(\omega)/E_{\mathrm{film}}(\omega)$. E_0 is equal to 80 kV/cm. Lines indicate the corresponding calculation using the classical anharmonic oscillator model with quartic anharmonicity and nonlinear dephasing. Arrows indicate zero-crossings and peaks of real and imaginary parts, respectively, which correspond approximately to the resonant frequencies.

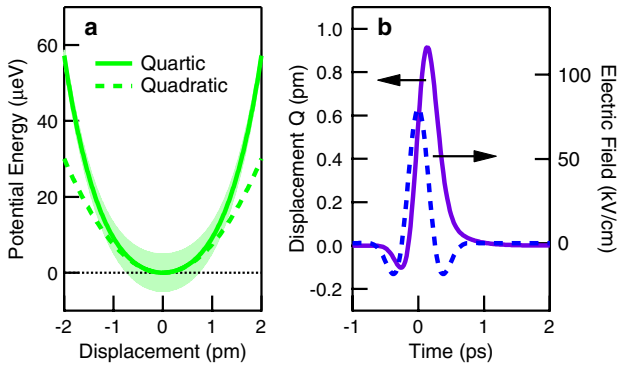

FIG. 3 (color online). (a) Potential curve of the anharmonic soft-mode potential used in the simulation. Broken line indicates the harmonic part. The width of the potential schematically indicates the corresponding dephasing rate, which depends on the displacement. (b) Calculated displacement of the soft mode for $E_0 = 80$ kV/cm. Incident electric field used in the calculation is also indicated by a broken line.

which causes variations in the quadratic term of the local potential, leading in turn to the observed inhomogeneous broadening in the linear spectrum. The negative nonlinear damping coefficient α indicates that when the induced displacement of the soft mode is much larger than that due to inhomogeneities, contributions from higher-order terms of the potential become dominant and the variations in the potential decrease. As shown in Fig. 3(a), the inhomogeneous broadening is large at the potential minima of the potential, whereas it decreases at larger displacements.

Figure 3(b) shows the calculated displacement of the soft mode under the application of terahertz waves having a peak field amplitude E_0 of 80 kV/cm. The calculation shows that the terahertz pulses coherently drive the displacement of the soft mode to 1 pm, which is only 1 order of magnitude smaller than the displacement associated with the ferroelectric phase transition in related ferroelectric materials such as $BaTiO_3$ (~ 10 pm) [29]. Considering the difference between the Curie temperatures of $BaTiO_3$ (393 K) and $SrTiO_3$ (35.5 K [9]), the ferroelectric displacement in the perturbation-induced ferroelectric phase in $SrTiO_3$ is expected to be smaller than that in $BaTiO_3$. Therefore, the amplitude of the induced displacement can be regarded as comparable to that of the ferroelectric phase transition in $SrTiO_3$, which is sufficiently large to show a nonlinear response due to anharmonicity.

The obtained quartic anharmonicity constant λ can be compared to the thermodynamic quartic anharmonicity constant β in Ref. [30], which is the coefficient of the $\beta P^4/4$ term in the free energy (P is the polarization). From our experiment, β ($= M\lambda/N^3e^{*4}$) is estimated to be 1×10^{11} J m^5 C^{-4}, which is 1 order of magnitude higher than the reported value of β [30]. One possible reason for this discrepancy can be explained as follows: Interactions slower than the terahertz periodicity cannot contribute to the nonlinear response of the soft mode, although they can contribute to reducing the nonlinearity in the thermodynamic static-field experiment. The higher-order terms in the soft-mode potential could also affect the quartic anharmonicity value estimated in our experiment because we neglected them in the simulation for simplicity. These results suggest that nonlinear terahertz spectroscopy is an indispensable tool for understanding the intrinsic anharmonic lattice dynamics in materials.

Our results confirmed that the terahertz pulses drive the soft mode to larger displacements than those induced by inhomogeneities and that intrinsic anhamonicity is observed. Since this method can probe the intrinsic anharmonicity at a fixed temperature, similar experiments on ferroelectric or quantum paraelectric bulk crystals could advance our understanding of the novel anharmonic lattice dynamics of the soft mode, such as quantum paraelectricity and quantum ferroelectricity. Additionally, the ability to tune the dielectric properties of $SrTiO_3$ thin films by changing the substrate [31,32] may enable the investigation of the nonlinear dynamics for various potential shapes, including double wells.

In summary, we demonstrated that intense monocycle terahertz pulses can impulsively drive the dipole of the soft mode in a $SrTiO_3$ thin film to large displacements. The soft mode exhibits a nonlinear response owing to the anharmonicity, that is, the blueshift and spectral narrowing. The induced displacement exceeds that due to inhomogeneities in the thin film, and becomes comparable to that of the perturbation-induced ferroelectric phase transition. These nonlinear responses can be interpreted using a classical anharmonic oscillator model, thus allowing quantitative measurement of the strong intrinsic quartic anharmonicity of the soft mode in a $SrTiO_3$ thin film and the nonlinear damping. The coherent driving of the collective mode to the anharmonic region demonstrated in this study could open an interesting new pathway to coherent control of macroscopic phases in condensed matter.

This work was partially supported by the Ministry of Education, Culture, Sports, Science and Technology through KAKENHI (Grants No. 21104510, No. 20241025, No. 23241034, and No. 20104007). I. K. also acknowledges the financial support received through the Special Coordination Funds for Promoting Science and Technology from the Japan Science and Technology Agency (JST).

[1] *Photoinduced Phase Transitions*, edited by K. Nasu (World Scientific, Singapore, 2004).
[2] K. Sokolowski-Tinten, C. Blome, J. Blums, A. Cavalleri, C. Dietrich, A. Tarasevitch, I. Uschmann, E. Förster, M. Kammler, M. von Hoegen, and D. von der Linde, Nature (London) **422**, 287 (2003).
[3] A. Assion, T. Baumert, M. Bergt, T. Brixner, B. Kiefer, V. Seyfried, M. Strehle, and G. Gerber, Science **282**, 919 (1998).

[4] S. Iwai, S. Tanaka, K. Fujinuma, H. Kishida, H. Okamoto, and Y. Tokura, Phys. Rev. Lett. **88**, 057402 (2002).
[5] M. Hase, M. Kitajima, S. Nakashima, and K. Mizoguchi, Phys. Rev. Lett. **88**, 067401 (2002).
[6] C. J. Brennan and K. A. Nelson, J. Chem. Phys. **107**, 9691 (1997).
[7] T. Qi, Y.-H. Shin, K.-L. Yeh, K. A. Nelson, and A. M. Rappe, Phys. Rev. Lett. **102**, 247603 (2009).
[8] M. Jewariya, M. Nagai, and K. Tanaka, Phys. Rev. Lett. **105**, 203003 (2010).
[9] K. A. Müller and H. Burkard, Phys. Rev. B **19**, 3593 (1979).
[10] P. A. Fleury and J. M. Worlock, Phys. Rev. **174**, 613 (1968).
[11] H. Uwe and T. Sakudo, Phys. Rev. B **13**, 271 (1976).
[12] M. Itoh, R. Wang, Y. Inaguma, T. Yamaguchi, Y.-J. Shan, and T. Nakamura, Phys. Rev. Lett. **82**, 3540 (1999).
[13] J. A. S. Barker, Phys. Rev. **145**, 391 (1966).
[14] H. Vogt, Phys. Rev. B **51**, 8046 (1995).
[15] M. Misra, K. Kotani, I. Kawayama, H. Murakami, and M. Tonouchi, Appl. Phys. Lett. **87**, 182909 (2005).
[16] I. Katayama, H. Shimosato, D. S. Rana, I. Kawayama, M. Tonouchi, and M. Ashida, Appl. Phys. Lett. **93**, 132903 (2008).
[17] A. A. Sirenko, C. Bernhard, A. Golnik, A. M. Clark, J. Hao, W. Si, and X. X. Xi, Nature (London) **404**, 373 (2000).
[18] Y. Ichikawa, M. Nagai, and K. Tanaka, Phys. Rev. B **71**, 092106 (2005).
[19] J. Hebling, G. Almási, I. Kozma, and J. Kuhl, Opt. Express **10**, 1161 (2002).
[20] M. Jewariya, M. Nagai, and K. Tanaka, J. Opt. Soc. Am. B **26**, A101 (2009).
[21] J. Hebling, K.-L. Yeh, M. C. Hoffmann, and K. A. Nelson, IEEE J. Sel. Top. Quantum Electron. **14**, 345 (2008).
[22] M. Nagai, M. Jewariya, Y. Ichikawa, H. Ohtake, T. Sugiura, Y. Uehara, and K. Tanaka, Opt. Express **17**, 11 543 (2009).
[23] J. J. Tu, C. C. Homes, and M. Strongin, Phys. Rev. Lett. **90**, 017402 (2003).
[24] M. Tinkham, Phys. Rev. **104**, 845 (1956).
[25] A. Yamanaka, M. Kataoka, Y. Inaba, K. Inoue, B. Hehlen, and E. Courtens, Europhys. Lett. **50**, 688 (2000).
[26] T. Hattori, J. Chem. Phys. **133**, 204503 (2010).
[27] W. Zhong, R. D. King-Smith, and D. Vanderbilt, Phys. Rev. Lett. **72**, 3618 (1994).
[28] B. U. Felderhof and G. Marowsky, Appl. Phys. B **43**, 161 (1987).
[29] R. E. Cohen, Nature (London) **358**, 136 (1992).
[30] C. Kadlec, F. Kadlec, H. Němec, P. Kůzel, J. Schubert, and G. Panaitov, J. Phys. Condens. Matter **21**, 115902 (2009).
[31] J. H. Haeni, P. Irvin, W. Chang, R. Uecker, P. Reiche, Y. L. Li, S. Choudhury, W. Tian, M. E. Hawley, B. Craigo, A. K. Tagantsev, X. Q. Pan, S. K. Streiffer, L. Q. Chen, S. W. Kirchoefer, J. Levy, and D. G. Schlom, Nature (London) **430**, 758 (2004).
[32] N. A. Pertsev, A. K. Tagantsev, and N. Setter, Phys. Rev. B **61**, R825 (2000).